Glacier sensitivity to equilibrium line altitude and reconstruction for the Last Glacial cycle: glacier modeling in the Payuwang Valley, western Nyaiqentanggulha Shan, Tibetan Plateau

Xu, Xiangke; Glasser, Neil

Published in:
Palaeogeography, Palaeoclimatology, Palaeoecology

DOI:
10.1016/j.palaeo.2015.09.025

Publication date:
2015

Citation for published version (APA):
Xu, X., & Glasser, N. (2015). Glacier sensitivity to equilibrium line altitude and reconstruction for the Last Glacial cycle: glacier modeling in the Payuwang Valley, western Nyaiqentanggulha Shan, Tibetan Plateau. *Palaeogeography, Palaeoclimatology, Palaeoecology*. https://doi.org/10.1016/j.palaeo.2015.09.025

Accepted Manuscript

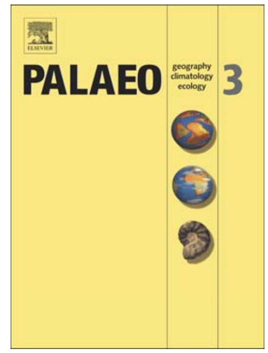

Glacier sensitivity to equilibrium line altitude and reconstruction for the Last Glacial cycle: glacier modeling in the Payuwang Valley, western Nyaiqentanggulha Shan, Tibetan Plateau

Xiangke Xu, Neil F. Glasser

PII: S0031-0182(15)00535-0
DOI: doi: 10.1016/j.palaeo.2015.09.025
Reference: PALAEO 7472

To appear in: *Palaeogeography, Palaeoclimatology, Palaeoecology*

Received date: 16 October 2014
Revised date: 6 September 2015
Accepted date: 16 September 2015

Please cite this article as: Xu, Xiangke, Glasser, Neil F., Glacier sensitivity to equilibrium line altitude and reconstruction for the Last Glacial cycle: glacier modeling in the Payuwang Valley, western Nyaiqentanggulha Shan, Tibetan Plateau, *Palaeogeography, Palaeoclimatology, Palaeoecology* (2015), doi: 10.1016/j.palaeo.2015.09.025

Glacier sensitivity to equilibrium line altitude and reconstruction for the Last Glacial cycle: glacier modeling in the Payuwang Valley, western Nyaiqentanggulha Shan, Tibetan Plateau

Xiangke Xu [a, b, *], Neil F. Glasser [b]

[a] *Key Laboratory of Tibetan Environment Changes and Land Surface Processes, Institute of Tibetan Plateau Research, CAS, Beijing 100101, China*

[b] *Centre for Glaciology, Department of Geography and Earth Sciences, Aberystwyth University, Aberystwyth SY233DB, UK*

Abstract

Glaciers respond sensitively to climate change and paleoclimate conditions can be inferred from the geomorphic evidence by reconstructing equilibrium line altitude (*ELA*) and by modeling glacier mass balance and ice flow. However, such work has not been extensively carried out on the vast Tibetan Plateau, and thus the knowledge of glacier sensitivity to paleoclimate change and paleoglacier volume is still lacking on the plateau. Recent improvements in understanding glacial extent and chronology in the Payuwang Valley, southern Tibetan Plateau present an opportunity to estimate the paleoclimate conditions during the Last Glacial cycle. Using a coupled mass-balance and ice-flow model, this study tests the glacier sensitivity to *ELA* change in the Payuwang Valley. By fitting modeled glaciers to the corresponding moraine positions, we reconstruct glacier extents probably occurred at oxygen isotope stage 3 (MIS 3) and Last Glacial Maximum (LGM) in the valley and infer the related climate conditions that could have supported these glacier advances. The glacier sensitivity tests indicate that in the Payuwang Valley the glaciers responded to centennial-scale shifts in climate. With ELAs below 5600 m asl, the tributary glaciers coalesce into the main valley and expand rapidly there. The model results also show that the Payuwang

Valley contained ice volumes of ~1.58×10^9 m^3 and ~1.23×10^9 m^3 with *ELA* lowering values of 370 m and 340 m in the MIS 3 and LGM glacial advances, respectively. By examining other independent paleoclimatic reconstructions, we conclude that during the MIS 3 glacier advance the temperature was only 1.5°C lower or even 0.2°C higher than the period of 2005-2008 with precipitation 40-100% higher than the 2005-2008 amount; and during the LGM glacier advance the temperature was 3.3-4.4°C lower than the period of 2005-2008 with the precipitation 30-70% lower than the 2005-2008 amount. These estimates add to the knowledge of better understanding the relationship between glacier dynamic and climatic change on the Tibetan Plateau.

***Keywords*:** Payuwang Valley; Last Glacial Maximum (LGM); equilibrium line altitude (*ELA*); glacier modeling; paleoclimate

* Corresponding author: xkxu@itpcas.ac.cn (X. Xu); TEL: +861084097114.

1. Introduction

Glacier fluctuations over time give some of the clearest evidence of climate change because their mass balance and areal extent are primarily determined by climate (Oerlemans, 2001; IPCC, 2013). Therefore, paleoclimatic inferences can be made by reconstructing the timing and extent of past mountain glaciers, which is of primary importance in understanding the climate processes and thresholds responsible for glacier mass balance variations.

Throughout the Tibetan Plateau, accurate documentation of past glacier fluctuations has been aided by cosmogenic ^{10}Be exposure dating since the late twentieth century (e.g., Phillips et al., 2000; Owen et al., 2008; Owen and Dortch, 2014; Chevalier et al., 2011; Heyman, 2014). For example, recent papers documenting Quaternary glaciations on the Tibetan Plateau on the basis of ^{10}Be-dated moraines show that during the Last Glacial cycle, glacier fluctuations across the Tibetan Plateau were heterogeneous (Owen and Dortch, 2014; Heyman, 2014). Even though these studies provide precious information on glacier fluctuations, little attention has been paid to reconstructing glaciological parameters such as glacier mass balance and ice volume which are essential to recognize water resource evolution in a mountain region.

Although temperature and precipitation are important climatic controls on glacier extent, the relationship between glacier and climate is complex, and there is no simple function connecting glacier fluctuations to the climate forcing. The equilibrium line altitude (*ELA*) on a glacier is a theoretical altitude where glacier accumulation equals ablation (net balance is zero). The accumulation is highly influenced by the regional distribution of precipitation as snow and local redistribution of snow by avalanching and/or wind (the latter can locally increase the accumulation and thus depress the *ELA* below the actual one); and the ablation is related to the processes of evaporation, melting of snow and ice, radiation and heat exchange with the air (e.g., Ohmura et al., 1992; Dahl and Nesje, 1992; Lie et al., 2003). In addition, glacier topography and aspect may have a local influence on the *ELA* (e.g., Porter, 1975; Dahl and Nesje, 1992; Benn et al., 2005). However, the main parameters controlling the *ELA* are the regional temperature and precipitation as snow. Therefore, the *ELA* is considered as a useful parameter to quantify the influence of climatic changes on glaciers, and its variability is widely used to compare glacier changes between different locations and infer past climatic conditions (e.g., Porter, 1975; Kuffey and Paterson, 2010; Benn et al., 2005).

Traditionally, paleotemperatures inferred from glacial records are based on the assumption that a lowering of glacier *ELA* is solely the result of temperature decrease associated with the atmospheric lapse rate (Hostetler and Clark, 2000). Some efforts have been made to relate the *ELA* change to both temperature and precipitation (Ohmura et al., 1992; Seltzer, 1994; Lie et al., 2003; Xu et al., 2010). However, large uncertainties remain in the estimation of past-glacier *ELA* using the traditional geomorphic methods, such as Area Accumulation Ratio (AAR), Terminus to Headwall Altitude Ratio (THAR) and Area Weighted Mean (AWM) methods. This is at least partly attributed to the large ranges of these empirical parameters in different mountain regions, which makes it difficult to select realistic values when calculating the paleo-ELA for any one specific valley. Apart from the attempt to infer *ELA* from the empirical-parameter methods, full numerical modelling of the past glacier extent is an alternative method to retrieve the paleo-ELA (Xu et al., 2013; 2014). Using the glacier modelling method, Xu et al. (2014) have simulated glacier extents during the Last Glacial cycle in the Tashkurgan catchment, northwestern Tibetan Plateau and inferred the glacier parameters (including paleo-ELAs) and climatic conditions that supported the glacier advances. Such modeling work carried out in different parts of the vast Tibetan Plateau can help to fully understand the relationships between glacier fluctuations and climatic changes in the region.

This study focuses on the northern slope of the western Nyaiqentanggulha Shan, which lies on southern Tibetan Plateau, (Fig. 1). The western Nyaiqentanggulha Shan stretches about 250 km from SW to NE and includes more than thirty peaks over 6000 m asl, with the highest Nyaiqentanggulha peak at 7117 m asl (Yu et al., 2013). During the Late Quaternary, the western Nyaiqentanggulha Shan was intensively glaciated, and many moraines were formed and well preserved in the glaciated valleys (Li et al., 1986). Recently, the nature and timing of the Quaternary glaciations of the mountains have been studied using geomorphologic investigations and cosmogenic ^{10}Be exposure dating methods (Owen et al., 2005; Chevalier et al., 2011; Dong et al., 2014). These studies indicate that in the area, glaciers advanced at least two times during the Last Glacial cycle. Such improvement in understanding the glacial chronologies and glacier variations provides a framework for modeling glacier extents and inferring related climatic changes. In addition, quantitative reconstructions of the regional climate for the Last Glacial cycle are still sparse in the western Nyaiqentanggulha Shan (Miehe et al., 2011; Schmidt et al., 2011). Here we use a numerical glacier model to simulate glacier extents in the Payuwang Valley and test the glacier sensitivity to climatic (ELA) changes.

2. Study area

The Payuwang Valley (30.5°N, 90.7°E) originates from a peak at 5820 m asl and drains a ~30-km^2 catchment into the Nam Co (Co means 'lake' in local language) on the northern side of the western Nyaiqentanggulha Shan (Fig. 1, Fig. 2A).The south

Asian monsoon, carrying moisture from the India Ocean, dominates in summer; and the westerlies derived from the Mediterranean Sea and/or the Atlantic Ocean dominate in winter (Yatagai and Yasunari, 1998; Shi, 2002). This produces a distinct seasonal oscillation of the climate with warm-wet summers (May-September) and cold-dry winters (October-April). Local moisture recycling, especially from the Nam Co, also contributes to the moisture transportation in the region (Yu et al., 2008). Observations at Nam Co Station (30°46.44'N, 90°59.31'E, 4730 m asl), indicate that the mean annual temperature was 0°C and the mean annual precipitation was 282 mm in the period 2005-2006, with more than 90% of the precipitation delivered between May and September (You et al., 2007). The *ELA* rises from ~5600 m asl on the southeastern slopes to ~5800 m asl on the northwestern slopes in the area. This reflects the controls of the south Asia monsoon penetrating this region and the orographic effects (windward/leeward slopes) on the variability of regional *ELA* (Li et al., 1986; Shi et al., 2009).

The Payuwang valley extends down 13.5 km to an elevation of 4750 m asl, and its floor slopes gently (<5°) towards the north. Within the valley, there are only two small modern hanging glaciers with a total area less than 0.5 km. Two lateral-terminal moraines are well preserved near the mouth of the valley (Dong et al., 2014). The outer moraine extends ~1.6 km downstream from the mouth of the Payuwang Valley and its altitude ranges from 4790 to 4950 m asl. The inner moraine, rising 3-5 m above the present river, is present within 0.5 km of the valley mouth and has an altitude range from 4920 to 4950 (Fig. 2A). Accordingly, this paper focuses on simulating the respective glacier extents constrained by the two moraines and estimating the ELAs for these glacier advances.

Using cosmogenic ^{10}Be exposure dating, Dong et al. (2014) dated 5 and 10 boulder samples for the outer and inner moraines respectively. The ages on the inner moraine (18.0±1.7 to 30.6±2.8 ka) are more overlapping than those on the outer moraine (18.0±1.6 to 39.9±3.7 ka). For the ages on the inner moraine, Dong et al. (2014) calculated the mean age to be 23.8±4.0 ka and obtained the highest-probability age of ~23.5 ka using a probability-density-function method. For the wider-spread ages on the outer moraine, Dong et al. (2014) tended to choose the maximum age of 39.9±3.7 ka to represent the minimum age of this glaciation, considering that incomplete exposure is the main factor causing exposure age scatter (Heyman et al., 2011). Using an updated global reference ^{10}Be production rate and a more robust statistical method, Heyman (2014) recalculated the ages for the two glaciations. Heyman (2014, in Appendix file) showed that the inner and outer moraines respectively have a deglaciation age of 25.9±3.9 ka and 38.6±15.3 ka. The age of 25.9±3.9 ka closely overlaps with the 23.8±4.0 ka by Dong et al. (2014) and these ages have a relatively small uncertainty (~4.0 ka). This gives us much confidence to believe that the inner moraine represents the global Last Glacial Maximum (LGM). In addition, from a morphostratigraphic view and weathering features, it is clear that the outer moraine is older than the inner moraine (detailed geomorphologic description for the two moraines can be seen in Dong et al. (2014)). Although it is difficult to rule out the possibility that the outer moraine formed during the marine oxygen isotope stage (MIS) 4 glacial stage, more and more ^{10}Be dating evidence showed that the glaciers advanced during the MIS 3 (60-30 ka) in the region influenced by the Asia summer monsoon, such as Himalaya, Anyemaqen, Nianbaoyeze, and Qilian mountains (e.g., Finkel et al., 2003; Owen et al., 2003; Wang et al., 2013; Murari et al., 2014; Owen and Dortch, 2014). Accounting for these evidence, combined with the ages by Dong et al. (2014) and Heyman (2014), we argue that the outer moraine corresponds to a glacier advance in MIS 3.

3. Modeling method

The model used is a combination of a surface mass balance model described by Zhao et al. (2014) in the region, and a two-dimensional shallow ice-flow model developed by Plummer and Phillips (2003). The annual surface mass balance (*SMB*) is a function of altitude (z) and *ELA*:

$$SMB(z) = \begin{cases} \beta_1(z - ELA - 170) + 170\beta_2 & z > ELA + 170 \\ \beta_2(z - ELA) & ELA - 40 \le z \le ELA + 170 \\ \beta_3(z - ELA + 40) - 40\beta_2 & z < ELA - 40 \end{cases} \quad (1)$$

Where β_1, β_2, β_3 are 0.6, 13, 5, respectively. The unit of *SMB* and β_i (i=1, 2, 3) here is mm a^{-1} (ice equivalent, i.e.) and a^{-1}, respectively. The mass balance result is then input to the ice-flow model to determine the corresponding glacier extent.

The ice-flow model was fully described in Plummer and Phillips (2003), and thus only a brief description is given here. The basic equation in the ice-flow model is the continuous equation for mass conservation expressed as follow:

$$\frac{\partial h}{\partial t} = SMB - \frac{\partial q_x}{\partial x} - \frac{\partial q_y}{\partial y} \quad (2)$$

Where h is the ice surface elevation, t is time, and q_x (q_y) is the ice flux along x (y) direction in the horizontal plane. The flux of ice between adjacent cells (q_x, q_y) is determined by the thickness, H, and the vertically-averaged flow velocity, u. The latter includes ice deformation (u_d) and sliding (u_s), and is calculated from following equation:

$$u = u_d + u_s = \frac{2}{5}(1 - f)HA\tau^m + fB\tau^n \quad (3)$$

Where A and B are coefficients of ice deformation and sliding; H is ice thickness; f is a factor used to adjust the fraction of flow caused by ice sliding versus deformation, and τ is basal shear stress and expressed as:

$$\tau = \nabla \rho g H \qquad (4)$$

Where ρ is ice density and g is gravitational acceleration.

The ice-flow model was used to evolve the glacier geometry through time by calculating the ice velocity u on a square grid that is offset from the points at which ice thickness is known. The flux gradients were then used to calculate the updated ice thickness using a forward explicit time-step. Eq. (3) is numerically solved using fully explicit five-point finite differences (Plummer and Phillips, 2003). We used the model codes for our study area and set the model parameters of A and B to be 1×10^{-7} Pa^{-3} a^{-1} and 1.5×10^{-3} m Pa^{-3} a^{-1}, respectively, consistent with the values accepted by Plummer and Phillips (2003). In addition, we assume that the glacier deposits moraines when it is in or near equilibrium with specific climate conditions, and thus a steady-state ice-flow simulation represents a possible climate for the glacier extent.

The input data for the glacier-climate model include a digital elevation model (DEM) and *ELA*. The DEM, with a 30 m spatial resolution, was downloaded from the Geospatial Data Cloud of CAS (http://www.gscloud.cn/) and trimmed slightly beyond the watershed of the Payuwang Valley (model domain 26.3 km^2). According to Yu et al. (2013), the ELAs on the extant Zhadang and Gurenhekou glaciers in 2005-2008 are 5750 and 5780 m asl (four-year average), respectively. Selecting the nearest glacier of Zhadang to the Payuwang Valley, we take the *ELA* of 5750 m asl in 2005-2008 as a reference to calibrate the model. We first run multiple simulations under this *ELA* value, with different f values (from 0.1 to 1.0) in attempts to match observed glacier distribution. We find that if the f value is constrained to be between 0.2 and 0.6, the modeled modern glacier extents agree well with the observed glacier extent. We show the modeled *SMB* (Fig. 2B) and glacier distribution (Fig. 2C) under the *ELA* value in 2005-2008, which match well with the observed contemporary glacier distribution in the study area. For simplicity, we set the *f* value to be 0.5 for the paleo-glacier simulations. To infer the *ELA* for each glacial stage, we prescribe different *ELA*s and run the model to simulate different steady-state glacier extents. We compare the resulting glacier extents with the glacial geomorphologic features (Dong et al., 2014), and then we choose the corresponding *ELA* that supports the glacier advance in each glacial stage.

To test the glacier sensitivity to *ELA* change and to reconstruct the glacier extent during each glacial stage, we initiated the simulation with the *ELA* at 5800 m asl, approximating the highest altitude in the domain. The *ELA* was then lowered in increments of 50 m to allow the glacier to obtain a new steady state configuration. As the simulated glacier terminus approached the dated moraine positions, the *ELA* was lowered by 10-m intervals in subsequent simulations to get the best-fitting glacier for each of the two LGC stages in the Payuwang Valley.

4. Results

4.1 Glacier sensitivity to *ELA* change

The variability in simulated glacier terminal-altitudes, areas, thicknesses, and volumes resulting from sensitivities to different *ELAs* are presented here (Fig 3). In all simulations, the ice-flow model reached steady state within a maximum of 300 model years, in which the proportion of integrated mass balance over glacier area relative to the integrated accumulation rate over the glacier accumulation area is less than 2%, and the larger the modeled glacier was, the more time was needed for the model to achieve steady state.

The sensitivity of glacier terminal-altitude to change in *ELA* was nearly constant (highly linear), and the terminal-altitude increased by ~227 m with the *ELA* increasing by 100 m (Fig. 3A). However, the changes in glacier thickness, area, and volume varied with the *ELA*. With an *ELA* decrease of 100 m, the maximum ice thickness increased by ~99.4 m and ~33.6 m when the *ELA* was below and above 5550 m, respectively (Fig. 3B). Under the same conditions, the area increased by ~6.7 km^2 and ~1.7 km^2, and the volume increased by 8.2×10^8 m^3 and 7.5×10^7 m^3, with the *ELA* below and above 5600 m, respectively (Fig. 3C, D). In addition, the change in accumulation area ratio (AAR) also has a similar trend. With an *ELA* decrease of 100 m, the AAR increased by ~2.6% and ~0.7% when the *ELA* was below and above 5550 m, respectively (Fig. 3E). When the *ELA* was 5600 m asl, the model showed that the tributary glaciers in the head of the Payuwang Valley began to coalesce into the main valley. When the *ELA* continuously decreased from 5600 m asl, the glacier expanded greatly and rapidly in the main valley. Therefore, an *ELA* of 5600 m asl appears to be a threshold for the glacier fluctuation in the Payuwang Valley.

4.2 Reconstruction of glacier extents

During the *ELA*-lowering experiments the glacial margins monotonically descended in the Payuwang Valley. Below 5500 m asl, the *ELA* was lowered in 10 m increments, and the best-fitting *ELAs* were 5410 and 5380 m asl for the inner and outer moraines, respectively. Compared with a contemporary *ELA* of 5750 m asl (2005-2008), the *ELA* during the two glacial stages dropped by 340 m and 370 m, respectively. The modeled SMB and ice thickness are displayed in Fig.4 for the two glacial stages. For the glacial stage corresponding to the inner moraine (*ELA*=5410 m asl), the modeled glacier area was 18.6 km^2, occupying 70.7% of the model domain, with the AAR being 47.5%. The calculated volume was 1.23×10^9 m^3, and the maximum ice thickness was 240 m (Fig. 4A, B). In the glacial stage relating to the outer moraine (*ELA*=5380), the calculated glacier area was 20.7 km^2, with the AAR being 48.3%. The estimated ice volume was 1.58×10^9 m^3, and the maximum ice thickness was 262 m (Fig. 4C, D).

5. Discussion

5.1 Glacier sensitivity to climate change

The relationship between glacial extent and climate change is complex, and this makes it difficult to directly quantify glacier sensitivity to climate change. However, using the reconstructed ELA drops, it is possible to infer the response of the glacier to climate change. By analysis of the surface mass balance sensitivity to climate change on the Xibu glacier, 25 km west to the Payuwang Valley, Caidong and Sorteberg (2010) argued that a temperature change of 1°C or a precipitation change of 35% correspond to an *ELA* change of 140 m. Because the temperature and precipitation are the most important factors determining the *ELA*, we can empirically describe the relationship between *ELA* and climate change (temperature and precipitation) as:

$$ELA \approx ELA_0 + 140 \times \Delta T - 4 \times \Delta P \qquad (5)$$

Where ELA_0 is a known ELA in a reference period (for example, 5750 m asl in 2005-2008), and the ΔT (°C), ΔP (%) are temperature and precipitation perturbations relative to the reference period. Using equation (5) combined with the glacier sensitivity to *ELA*, we discuss the glacier sensitivity to climate change.

As mentioned above, the glacier terminal-altitude descends by ~227 m if the *ELA* drops by 100 m. Assuming precipitation is constant, this indicates that a temperature decrease of 1°C relative to the values of 2005-2008 can lead to a glacial terminal-altitude decrease of 318 m. Likewise, when the glaciers are located in the tributary valleys (*ELA* above 5600 m asl), a temperature decrease of 1°C can lead to glacier area and volume increases of 2.4 km^2 and 1.05×10^8 m^3, respectively. When the tributary glaciers coalesce and flow in the main valley (*ELA* below 5600 m asl), a temperature decrease of 1°C can lead to glacier area and volume increases of 9.4 km^2 and 1.15×10^9 m^3, respectively.

5.2 Climate conditions for the glacier advances during the Last Glacial cycle

By fitting modeled glaciers to the corresponding moraine positions, the *ELAs* were estimated to be 5380 and 5410 m asl for the glacier advances during MIS 3 and LGM, respectively. Using Eq (5), various combinations of ΔT (°C) and ΔP (%) can be inferred to support the glacier advances (Fig. 5). For example, assuming that during each of the two glacial stages, annual precipitation is equivalent to the value (ΔP =0) in 2005-2008, a temperature lowering (ΔT) of -2.4°C and -2.6°C is needed to reproduce the two glacial extents constrained by the inner and outer moraines, respectively. To better constrain the ranges of the ΔT and ΔP, it is necessary to examine other independent paleoclimatic reconstructions for each of the two glacial stages.

By compiling 75 paleoclimatic records (mainly lake and loess records), Herzschuh (2006) reconstructed the moisture evolution history in monsoonal central Asia over the last 50 ka and concluded that wet conditions occurred during middle and late MIS 3, while the LGM was characterized by dry climate conditions in the region. Prell and Kutzbach (1987) quantitatively estimated the precipitation change for southern Asia by considering the Northern Hemisphere summer radiation and glacial age boundary conditions. They argued that in the period between 75 and 15 ka, southern Asia was drier than today (weaker monsoon) with extensive ice sheet boundary conditions (MIS4 and LGM), and wetter in the interglacial period (MIS 3). In addition, from multiple lines of evidence including pollen, periglacial phenomena, and ice cores from the Tibetan Plateau, Shi et al. (1997, 2001) proposed that during the period 40-30 ka BP (MIS 3) precipitation was 40-100% higher than today, while during LGM the precipitation was 30-70% lower than today. By referencing these precipitation-related reconstructions, our study tentatively constrains *ΔP* values to be +40 to +100% and -30 to -70% for the MIS 3 and LGM, respectively. Considering these precipitation amounts, our model results suggest that a temperature of only 1.5°C lower or even 0.2°C higher than today is required to reproduce the MIS 3 glacial extents, and a temperature lowering of 3.3-4.4°C can support the LGM glacial extents in the Payuwang Valley.

The constrained *ΔT* ranges are comparable with some climate proxy results on the Tibetan Plateau. For example, by analysis of the pollen records from Lake Luanhaizi, northeast Tibetan Plateau, Herzschuh et al. (2006) reconstructed the temperature variability during the last 50 ka. Their results (Table 5 in their paper) suggested that the LGM climate was ~2.5-5.5°C colder than today (present mean annual temperature is -1°C at Lake Luanhaizi), and during some periods of MIS 3 the climate was only ~2.5°C colder or even 1.5°C warmer than today. Using terrestrial gastropod assemblages, Wu et al. (2002) argued that during the LGM a temperature lowering of 3-5°C occurred on the Chinese Loess Plateau. Furthermore, based on biogeographical data from ground beetles of the genus *Trechus*, and from private juniper tree haplotypes, Schmidt et al. (2011) suggested a maximum LGM temperature depression of 3-4°C in July for the southern Tibetan Plateau. Miehe et al. (2011) also argued that Alpine Steppes of Tibet persisted during the LGM with 3 to 4°C lower summer temperature, by hypothesizing that the Alpine Steppes of the Tibetan highlands remained ecologically stable during the LGM. Our results broadly overlap with these temperature estimates. However, from the $\delta^{18}O$ values of Guliya ice core, Shi et al. (2001) identified three climate phases during the MIS 3: around 55 ka, the temperature was 3°C higher than today; between 47-43 ka (MIS 3b, Shi and Yao, 2001), 5°C lower than today; and around 35 ka, 4°C higher than today. In addition, Shi et al. (1997) suggested that during the LGM, the mean annual temperature was 6-9°C lower than today. These $\delta^{18}O$-derived temperature values were estimated based on the quantitative relationship between the $\delta^{18}O$ value and temperature changes, that is, 1‰ drop in $\delta^{18}O$ represents a temperature lowering of about 1.6°C, and vice versa (Yao et al., 1995; Yao et al., 2006). These estimated temperature amplitudes are all larger than the corresponding estimates in this study. This may be caused by the mass balance model itself without directly accounting for the effects of solar radiation on melting rate. The mass balance model was formulated on the modern climate condition (Zhao et al., 2014), and thus it is especially suitable to infer temperature and precipitation during past interval when summer insolation was similar to modern. The summer insolation levels were lower and higher than present during the LGM and MIS 3 periods (Berger and Loutre, 1991). The lower insolation level may have caused a weaker monsoon in the region, contributing to the inferred lower -than-modern precipitation, and vice versa. This can lead to the estimated temperature amplitude less than its true value. On the other hand, the differences between our estimated temperature amplitudes and that from these climatic proxies may reflect the regional differences in the climate changes on the different parts of the vast Tibetan Plateau during same historical periods. Therefore, more modelling (especially accounting for effects of the changing insolation on surface mass balance) and proxy paleoclimatic reconstructions for the Last Glacial cycle are urgently needed to better understand the climate evolution on the vast Tibetan Plateau.

6. Conclusion

Using a coupled mass-balance and ice-flow model, we tested glacier sensitivity to *ELA* changes and inferred the climate conditions for the MIS 3 and LGM glacial advances in the Payuwang Valley by simulating the glacier advances that matched the corresponding observed moraines. The glacier sensitivity test indicated that the glaciers respond to centennial-scale shifts in climate and if the *ELA* is below 5600 m asl, the glacier expanded greatly and rapidly in the main valley. By fitting modeled glaciers to the corresponding moraine positions, the *ELAs* were estimated to be 5380 and 5410 m asl for the respective MIS 3 and LGM glacier advances, dropping by 370 m and 340 m relative to the present *ELA* (2005-2008). The model results showed that the Payuwang Valley was covered by glaciers of 20.7 km^2 and 18.6 km^2 and ice volumes of 1.58×10^9 m^3 and 1.23×10^9 m^3 in the MIS 3 and LGM glacial stages, respectively. By examining other independent paleoclimatic reconstructions, the study constrains the more realistic temperatures to be -0.2-1.5°C and 3.3-4.4°C lower than 2005-2008 that support the glacier extents during the MIS 3 and LGM glacial stages, respectively. These findings help to recognize the hydrological evolution in the region and benefit to understanding the relationships between glacier dynamic and climate change. We therefore stress that more paleoglacier-modeling work should be carried out on the vast Tibetan Plateau where abundant geomorphic features exist for past glacier changes.

Acknowledgments

This research was funded by the National Natural Science Foundation of China (NSFC, Grant No. 41471006, 41101004). We would like to thank Jakob Heyman and other two anonymous reviewers for their very helpful and thorough reviews of this paper. Also, many thanks to Guocheng Dong for providing useful moraine GPS data.

References

Benn, D.I., Owen, L.A., Osmaston, H.A., Seltzer, G.O., Porter, S.C., Mark, B., 2005. Reconstruction of equilibrium-line altitudes for tropical and sub-tropical glaciers. Quaternary International 138-139, 8-21.

Berger, A., Loutre, L.A., 1991. Insolation values for the climate of the last 10 million years. Quaternary Science Reviews 10, 297-317.

Caidong, C., Sorteberg, A., 2010. Modelled mass balance of Xibu glacier, Tibetan Plateau: sensitivity to climate change. Journal of Glaciology 56, 235-248.

Chevalier, M.-L., Hilley, G., Tapponnier, P., Van DerWeord, J., Liu-Zeng, J., Finkel, R.C., Ryerson, F.J., Li, H., Liu, X., 2011. Constraints on the late Quaternary glaciations in Tibet from cosmogenic exposure ages of moraine surface. Quaternary Science Reviews 30, 528-554.

Cuffey, K.M., Paterson, W.S.B., 2010. The Physics of Glaciers, fourth edition. Butterworth-Heinemann, Elsevier.

Dahl, S.O., Nesje, A., 1992. Paleoclimatic implications based on equilibrium-line altitude depressions of reconstructed Younger Dryas and Holocene cirque glaciers in inner Nordfjord, western Norway. Palaeogeography, Palaeoclimatology, Palaeoecology 94, 87-97.

Dong, G.C., Yi, C.L., Caffee, M., 2014. ^{10}Be dating of boulders on moraines from the last glacial period in the Nyainqentanglha mountains, Tibet. Science China (Earth Science) 57, 221-231.

Finkel, R.C., Owen, L.A., Barnard, P.L., Caffee, M.W., 2003. Beryllium-10 dating of Mount Everest moraines indicates a strong monsoonal influence and glacial synchroneity throughout the Himalaya. Geology 31, 561-564.

Herzschuh, U., 2006. Palaeo-moisture evolution in monsoon Central Asia during the last 50,000 years. Quaternary Science Reviews 25, 163-178.

Herzschuh, U., Kurschner, H., Mischke, S., 2006. Temperature variability and vertical vegetation belt shifts during the last ~50,000 yr in the Qilian Mountains (NE margin of the Tibetan Plateau, China). Quaternary Research 66: 133-146.

Heyman, J., 2014. Paleoglaciation of the Tibetan Plateau and surrounding mountains based on exposure ages and ELA depression estimates. Quaternary Science Reviews 91, 30-41.

Heyman, J., Stroeven, A.P., Harbor, J., Caffee, M.W., 2011. Too young or too old: evaluating cosmogenic exposure dating based on an analysis of compiled boulder exposure ages. Earth and Planetary Science Letters 302, 71-80.

Hostetler, S.W., Clark, P.U., 2000. Tropical climate at the last glacial maximum inferred from glacier mass-balance modeling. Science 290, 1747-1750.

IPCC, 2013. Climate Change 2013: The Physical Scientific Basis. Contribution of Working Group I to the Fifth Assessment Report of the Intergovernmental Panel on Climate Change (edited by: Stocker, T.F., Qin, D., Plattner, G.K.). Cambridge University Press.

Li, J., Zheng, B., Yang, X., Xie, Y., Zhang, L., Ma, Z., Xu, S., 1986. Glaciers in Tibet. Science Press, Beijing.

Lie, Ø., Dahl, S.O., Nesje, A., 2003. A theoretical approach to glacier equilibrium-line altitudes using meteorological data and glacier mass-balance records from southern Norway. The Holocene 13, 365-372.

Miehe, G., Miehe, S., Bach, K., Kluge, J., Wesche, K., Yang, Y., Liu, J., 2011. Ecological stability during the LGM and the mid-Holocene in the Alpine Steppes of Tibet? Quaternary Research 76, 243-252.

Murari, M.K., Owen, L.A., Dortch, J.M., Caffee, M.W., Dietsch, C., Fuchs, M., Haneberg, W.C., Sharma, M.C., Townsend-Small, A., 2014. Timing and climatic drivers for glaciation across monsoon-influenced regions of the Himalayan-Tibetan orogen. Quaternary Science Reviews 88, 159-182.

Oerlemans, J., 2001. Glaciers and Climate Change. A.A. Balkema, 148pp.

Ohmura, A., Kasser, P., Funk, M., 1992. Climate at the equilibrium line of glaciers. Journal of Glaciology 38: 397-411.

Owen, L.A., Caffee, M.W., Finkel, R.C., Seong, Y.B., 2008. Quaternary glaciation of the Himalayan-Tibetan orogen. Journal of Quaternary Science 23, 513-531.

Owen, L.A., Dortch, J.M., 2014. Nature and timing of Quaternary glaciation in the Himalayan-Tibetan orogen. Quaternary Science Reviews 88, 14-54.

Owen, L.A., Finkel, R.C., Barnard, P.L., Haizhou, M., Asahi, K., Caffee, M.W., Derbyshire, E., 2005. Climatic and topographic controls on the style and timing of Late Quaternary glaciation throughout Tibet and the Himalaya defined by ^{10}Be cosmogenic radionuclide surface exposure dating. Quaternary Science Reviews 24, 1391-1411.

Owen, L.A., Finkel, R.C., Ma, H., Spencer, J.Q., Derbyshire, E., Barnard, P.L., Caffee, M.W., 2003. Timing and style of late Quaternary glaciation in northeastern Tibet. Geological Society of America Bulletin 115, 1356-1364.

Phillips, W.M., Sloan, V.F., Shroder Jr., J.F., Sharma, P., Clarke, M.L., Rendell, H.M., 2000. Asynchronous glaciation at Nanga Parbat, northwestern Himalaya Mountains, Pakistan. Geology 28, 431-434.

Plummer, M.A., Phillips, F.M., 2003. A 2-D numerical model of snow/ice energy balance and ice flow for paleoclimatic interpretation of glacial geomorphic features. Quaternary Science Reviews 22, 1389-1406.

Porter, S.C., 1975. Equilibrium line altitudes of late Quaternary glaciers in the southern Alps, New Zealand. Quaternary Research 5, 27-47.

Prell, W.L., Kutzbach, J.E., 1987. Monsoon variability over the past 150,000 years. Journal of Geophysical Research 92, 8411-8425.

Schmidt, J., Opgenoorth, L., Martens, J., Miehe, G., 2011. Neoendemic ground beetles and private tree haplotypes: two independent proxies attest a moderate last glacial maximum summer temperature depression of 3-4 for the southern Tibetan Plateau. Quaternary Science Reviews 30, 1918-1925.

Seltzer, G.O., 1994. Climatic interpretation of Alpine snowline variations on millennial time scales. Quaternary Research 41, 154-159.

Shi, Y., 2002. Characteristics of Late Quaternary monsoon glaciation on the Tibetan Plateau and in East Asia. Quaternary International 97/98, 79-91.

Shi, Y., Liu, C., Kang, E., 2009. The glacier inventory of China. Annals of Glaciology 50, 1-4.

Shi, Y., Yao, T., 2002. MIS 3b (54－44ka BP) cold period and glacial advance in middle and low latitudes. Journal of Glaciology and Geocryology 21, 1-9 (in Chinese with English abstract).

Shi, Y., Yu, G., Liu, X., Li, B., Yao, T., 2001. Reconstruction of the 30-40 ka BP enhanced Indian Monsoon climate based on geological records from the Tibetan Plateau. Palaeogeography, Palaeoclimatology, Palaeoecology 160, 69-83.

Shi, Y., Zheng, B., Yao, T., 1997. Glaciers and environments during the Last Glacial Maximum (LGM) on the Tibetan Plateau. Journal of Glaciology and Geocryology 19: 97-113 (in Chinese with English Abstract).

Wang, J., Kassab, C., Harbor, J.M., Caffee, M.W., Cui, H., Zhang, G., 2013. Cosmogenic nuclide constraints on late Quaternary glacial chronology on the Dalijia Shan, northeastern Tibetan Plateau. Quaternary Research 79, 439-451.

Xu, X., Dong, G., Pan, B., 2014. Modeling glacier advances and related climate conditions during the last glaciation cycle in the Kuzigun Valley, Tashkurgan catchment on the northwest Tibetan Plateau. Journal of Quaternary Science, 29, 279-288.

Xu, X., Hu, G., Qiao, B., 2013. Last glacial maximum climate based on cosmogenic ^{10}Be exposure ages and glacier modeling for the head of Tashkurgan Valley, northwest Tibetan Plateau. Quaternary Science Reviews 80, 91-101.

Xu, X., Wang, L., Yang, J., 2010. Last Glacial Maximum climate inferences from integrated reconstruction of glacier equilibrium-line altitude for the head of the Urumqi River, Tianshan Mountains. Quaternary International 218, 3-12.

Yao, T., Jiao, K., Yang, Z., Shi, W., 1995. Climate change since the Little Ice Age in the Guliya ice core. Science in China (Series B) 25, 1108-1114 (in Chinese).

Yao, T., Wang, N., Shi, Y., Xu, B., Duan, K., Tian, L., 2006. Ice Core Study. In: Shi, Y. (Ed.), The Quaternary Glaciations and Environmental Variations in China. Hebei Science and Technology Publishing House, Shijiazhuang, pp. 12-62.

Yatagai, A., Yasunari, T., 1998. Variation of summer water vapor transport related to precipitation over and around the arid region in the interior of the Eurasian continent. Journal of Meteorological Society of Japan, 76(5), 799-815.

You, Q., Kang, S., Li, C., Li, M., Liu, J., 2007. Variation features of meteorological parameters at the Nam Co Station, Tibetan Plateau. Meteorology Monthly 33, 54-60 (in Chinese with English Abstract).

Yu, W., Yao, T., Kang, S., Pu, J., Yang, W., Gao, T., Zhao, H., Zhou, H., Li, S., Wang, W., Ma, L., 2013. Different region climate regimes and topography affect the changes in area and mass balance of glaciers on the north and south slopes of the same glacierized massif (the West Nyainqentanglha Range, Tibetan Plateau). Journal of Hydrology 495, 64-73.

Yu, W., Yao, T., Tian, L., Ma, Y., Ichiyanaki, K., Wang, Y., Sun, W., 2008. Relationship between $\delta^{18}O$ in precipitation and air temperature and moisture origin on a south-north transect of the Tibetan Plateau. Atmospheric Research 87, 158-169.

Zhao, L., Tian, L., Zwinger, T., Ding, R., Zong, J., Ye, Q., Moore, J.C., 20132014. Numerical simulations of Gurenhekou Glacier on the Tibetan Plateau. Journal of Glaciology 60, 71-82.

Captions for figures

Fig. 1. Location of the study area on the northern slope of the western Nyaiqentanggulha Shan, southern Tibetan Plateau, showing the model domain used in the coupled mass-balance and ice-flow model (enclosed by red line).

Fig. 2. (A) Geomorphologic map showing small contemporary glaciers and the large moraines formed during the LGM and MIS 3 in the Payuwang Valley (adapted from Dong et al., 2014); (B) modeled Surface Mass Balance (SMB) and (C) ice thickness with an *ELA* of 5750 m asl in the period of 2005-2008. Note that the modeled ice extent matches well with the observed glacier distribution. The units for SMB are meters of water in ice equivalents (i.e).

Fig. 3. The sensitivity tests of glacier parameters to the assumed *ELAs* in the Payuwang Valley: (A) glacier terminal altitude, (B) maximum ice thickness, (C) glacier area, (D) glacier volume, (E) glacier accumulation area ratio (AAR).

Fig. 4. Simulated glacier surface mass balance (SMB) and ice thickness for the LGM (Panels A and B) and MIS 3 glacial stages (panels C and D) with the *ELA* at 5410 m asl and 5380 m asl, respectively.

Fig. 5. Plot of temperature and precipitation combinations that respectively support the MIS 3 (*ELA*=5380 m asl) and LGM (*ELA*=5410 m asl) glacier extents.

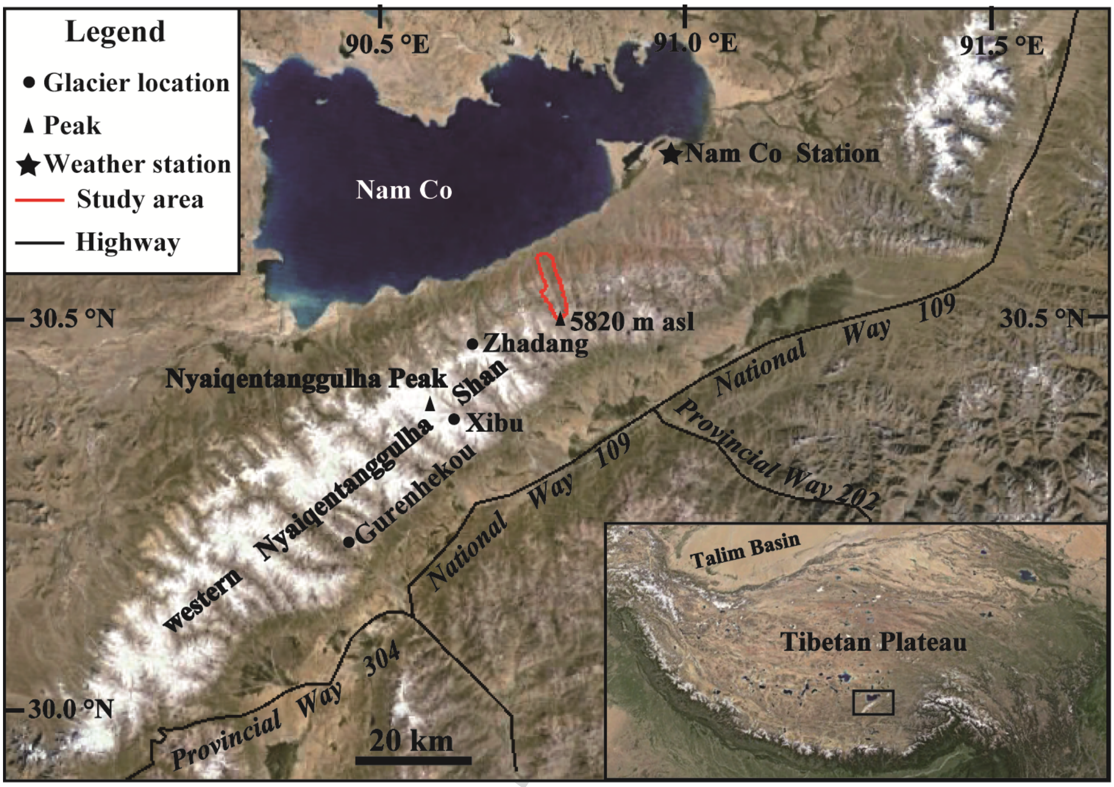

Legend
Glacier location
Peak
Weather station
Study area
Highway
90.5 °E
91.0 °E
91.5 °E
30.5 °N
30.0 °N
Nam Co
Nam Co Station
5820 m asl
Zhadang
Nyaiqentanggulha Peak
Xibu
Gurenhekou
western Nyaiqentanggulha Shan
National Way 109
Provincial Way 202
Provincial Way 304
20 km
Talim Basin
Tibetan Plateau

Fig. 1

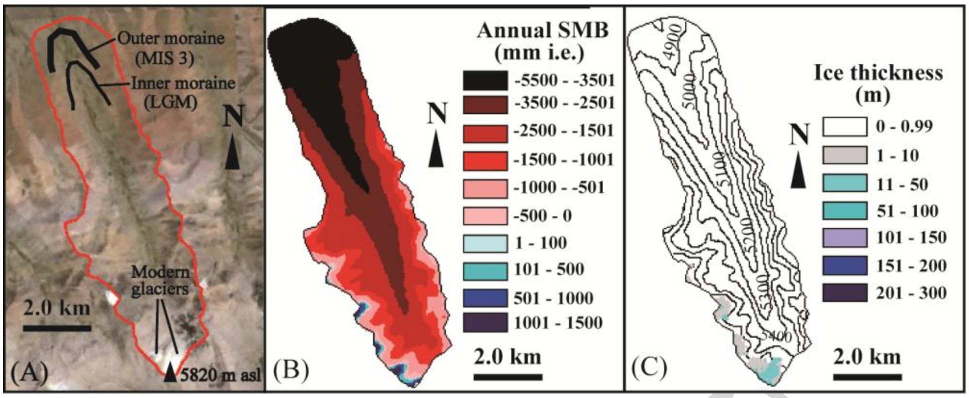
Outer moraine
(MIS 3)
Inner moraine
(LGM)
N
Modern
glaciers
2.0 km
(A)
5820 m asl
Annual SMB
(mm i.e.)
-5500 - -3501
-3500 - -2501
-2500 - -1501
-1500 - -1001
-1000 - -501
-500 - 0
1 - 100
101 - 500
501 - 1000
1001 - 1500
N
2.0 km
(B)
Ice thickness
(m)
0 - 0.99
1 - 10
11 - 50
51 - 100
101 - 150
151 - 200
201 - 300
4900
5000
5100
5200
5300
N
2.0 km
(C)

Fig. 2

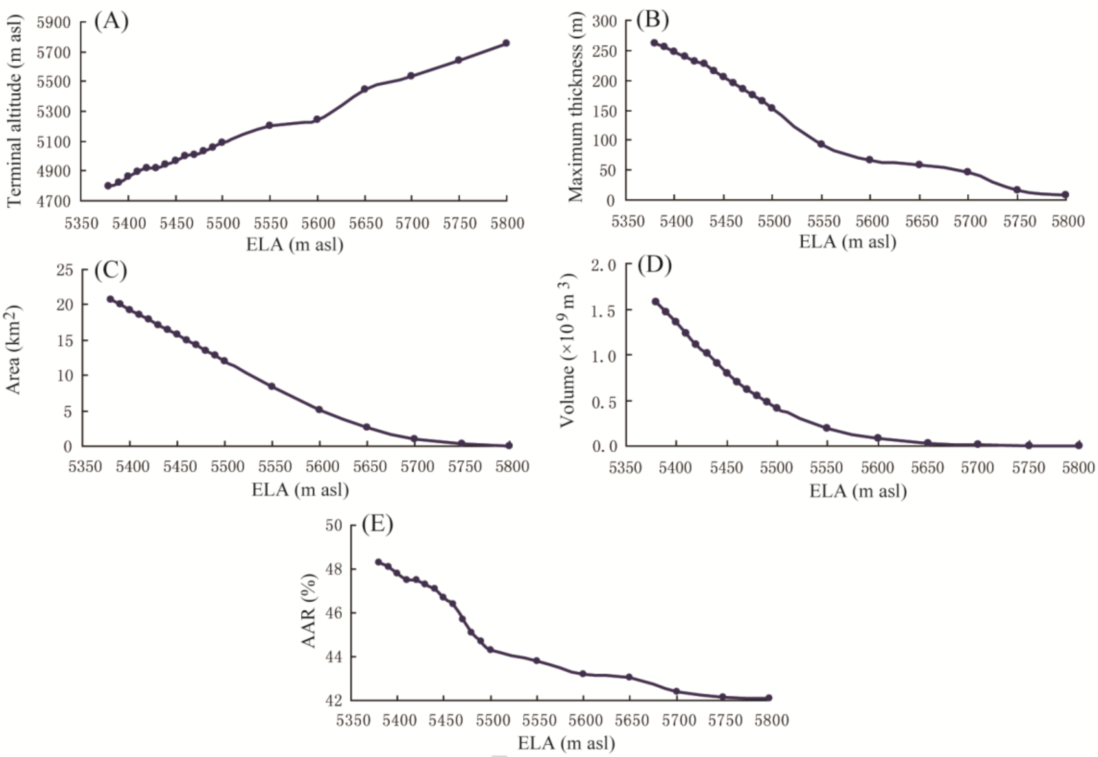
(A)
Terminal altitude (m asl)
5900
5700
5500
5300
5100
4900
4700
5350 5400 5450 5500 5550 5600 5650 5700 5750 5800
ELA (m asl)
(B)
Maximum thickness (m)
300
250
200
150
100
50
0
5350 5400 5450 5500 5550 5600 5650 5700 5750 5800
ELA (m asl)
(C)
Area (km2)
25
20
15
10
5
0
5350 5400 5450 5500 5550 5600 5650 5700 5750 5800
ELA (m asl)
(D)
Volume (×10⁹ m³)
2.0
1.5
1.0
0.5
0.0
5350 5400 5450 5500 5550 5600 5650 5700 5750 5800
ELA (m asl)
(E)
AAR (%)
50
48
46
44
42
5350 5400 5450 5500 5550 5600 5650 5700 5750 5800
ELA (m asl)

Fig. 3

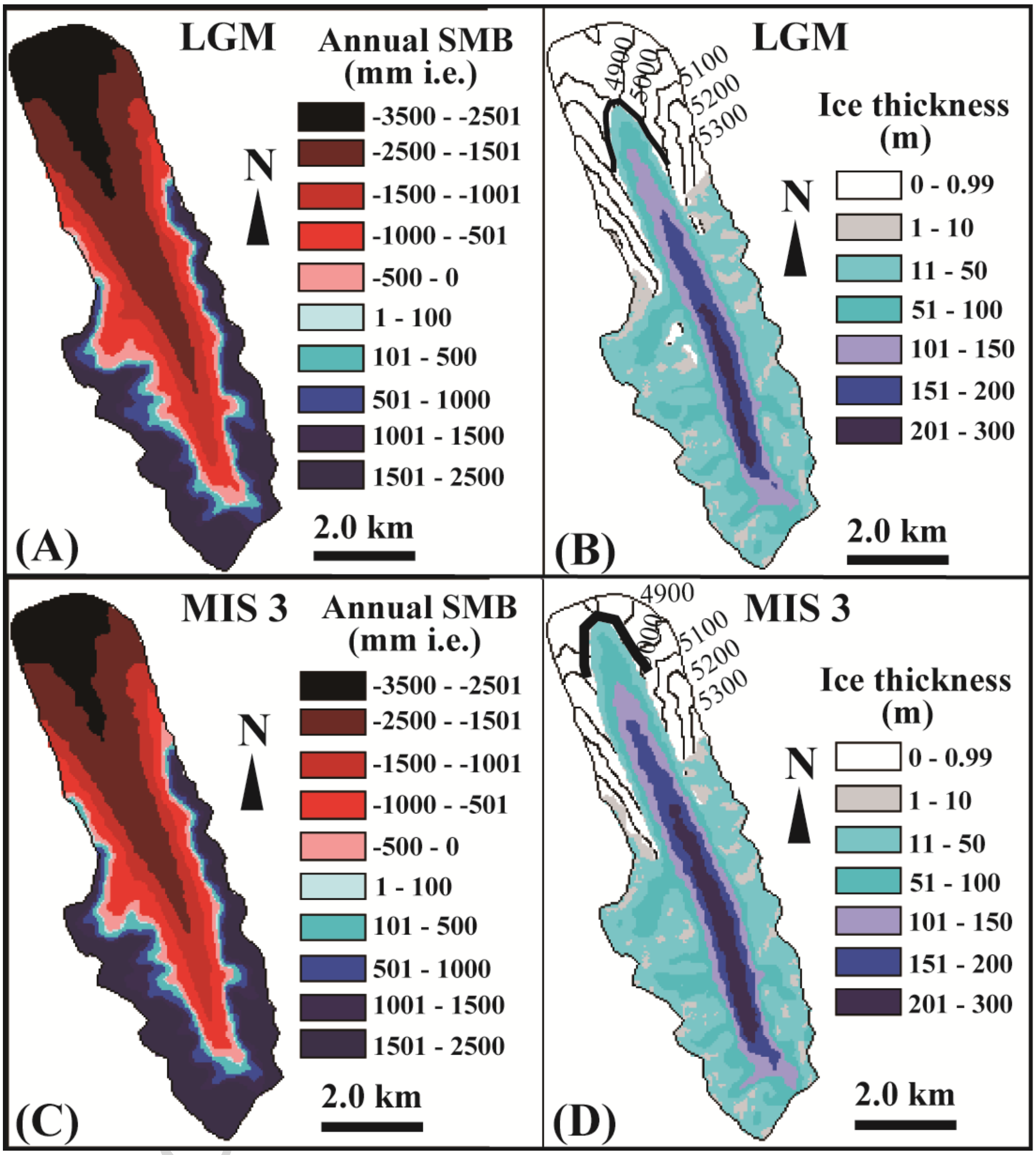
LGM
Annual SMB
(mm i.e.)
-3500 - -2501
-2500 - -1501
-1500 - -1001
-1000 - -501
-500 - 0
1 - 100
101 - 500
501 - 1000
1001 - 1500
1501 - 2500
N
2.0 km
(A)
LGM
4900
5000
5100
5200
5300
Ice thickness
(m)
0 - 0.99
1 - 10
11 - 50
51 - 100
101 - 150
151 - 200
201 - 300
N
2.0 km
(B)
MIS 3
Annual SMB
(mm i.e.)
-3500 - -2501
-2500 - -1501
-1500 - -1001
-1000 - -501
-500 - 0
1 - 100
101 - 500
501 - 1000
1001 - 1500
1501 - 2500
N
2.0 km
(C)
MIS 3
4900
5000
5100
5200
5300
Ice thickness
(m)
0 - 0.99
1 - 10
11 - 50
51 - 100
101 - 150
151 - 200
201 - 300
N
2.0 km
(D)

Fig. 4

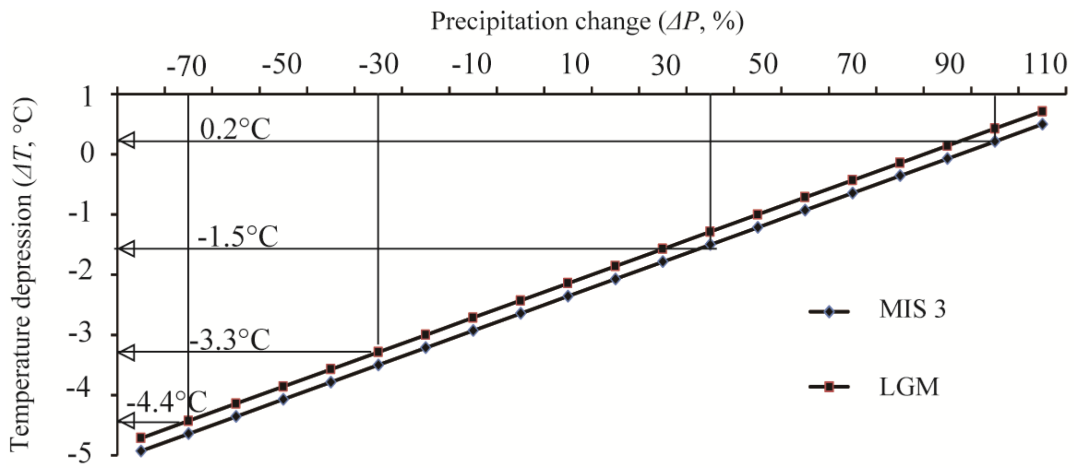

Fig. 5

Highlights

•A coupled mass-balance and ice-flow model was used
•Glacier sensitivity to ELA change was tested in a Tibet valley
•Glacier extents were reconstructed for the Last Glacial cycle
•Palaeoclimates that support the glacier extents were inferred